Casticin suppresses RANKL-induced osteoclastogenesis and prevents ovariectomy-induced bone loss by regulating the AKT/ERK and NF-κB signaling pathways

FAN YANG[1,2*], YUANGANG SU[1,3*], JIAMIN LIANG[1,3], KEYI WANG[1,2], HAOYU LIAN[1,3], JUNCHUN CHEN[1,3], JIAKE XU[4], JINMIN ZHAO[1,3] and QIAN LIU[1]

[1]Research Centre for Regenerative Medicine, Department of Orthopaedics, The First Affiliated Hospital of Guangxi Medical University; [2]Collaborative Innovation Centre of Regenerative Medicine and Medical BioResource Development and Application, Guangxi Medical University; [3]Guangxi Key Laboratory of Regenerative Medicine, Guangxi Medical University, Nanning, Guangxi 530021, P.R. China; [4]School of Biomedical Sciences, The University of Western Australia, Perth 6009, Australia

Received November 17, 2022; Accepted March 23, 2023

DOI: 10.3892/ijmm.2023.5246

Abstract. Postmenopausal osteoporosis is a systemic metabolic disease that chronically endangers public health and is typically characterized by low bone mineral density and marked bone fragility. The excessive bone resorption activity of osteoclasts is a major factor in the pathogenesis of osteoporosis; therefore, strategies aimed at inhibiting osteoclast activity may prevent bone decline and attenuate the process of osteoporosis. Casticin (Cas), a natural compound, has anti-inflammatory and antitumor properties. However, the role of Cas in bone metabolism remains largely unclear. The present study found that the receptor activator of nuclear factor-κB (NF-κB) ligand-induced osteoclast activation and differentiation were inhibited by Cas. Tartrate-resistant acid phosphatase staining revealed that Cas inhibited osteoclast differentiation, and bone resorption pit assays demonstrated that Cas affected the function of osteoclasts. Cas significantly reduced the expression of osteoclast-specific genes and related proteins, such as nuclear factor of activated T cells, cytoplasmic 1 and c-Fos at the mRNA and protein level in a concentration-dependent manner. Cas inhibited osteoclast formation by blocking the AKT/ERK and NF-κB signaling pathways, according to the intracellular signaling analysis. The microcomputed tomography and tissue staining of tibiae from ovariectomized mice revealed that Cas prevented the bone loss induced by estrogen deficiency and reduced osteoclast activity *in vivo*. Collectively, these findings indicated that Cas may be used to prevent osteoporosis.

Correspondence to: Professor Qian Liu or Professor Jinmin Zhao, Research Centre for Regenerative Medicine, Department of Orthopaedics, The First Affiliated Hospital of Guangxi Medical University, 6 Shuangyong Road, Nanning, Guangxi 530021, P.R. China
E-mail: liuqian@gxmu.edu.cn
E-mail: zhaojinmin@126.com

*Contributed equally

Key words: casticin, osteoclast, AKT, ERK, NF-κB, osteoporosis

Introduction

The human skeleton is a dynamic system (1). Osteoclasts, osteoblasts and osteocytes regulate bone mass, and the disruption of the balance of activity between these cells can result in bone diseases, such as osteoporosis and periodontal disease, which can severely endanger human health (2,3). Controlling the differentiation and functionality of these cells is thus crucial from a therapeutic standpoint. An imbalance in the activity of osteoclasts and osteoblasts caused by an increase in the quantity and function of osteoclasts as a result of estrogen deprivation is the hallmark of postmenopausal osteoporosis, a prevalent skeletal illness affecting older women (4,5). The course of postmenopausal osteoporosis can be attenuated by suppressing osteoclast formation and activity, according to pertinent studies (6,7).

Osteoclasts are known for their bone resorbing function and are a special type of terminally differentiated cell that originates from the blood lineage monocyte-macrophage system (8). Macrophage colony-stimulating factor (M-CSF) and receptor activator of nuclear factor κB (NF-κB) ligand (RANKL) control osteoclast formation (9,10). Multiple intracellular signaling events are activated by the interaction of RANKL with its receptor, RANK, which influences the function and survival of osteoclasts. These effectors stimulate the expression and activation of transcription factors, such as nuclear factor of activated T cells, cytoplasmic 1 (NFATc1), which is required for osteoclast precursor differentiation (11,12). The inhibition of the intracellular process that is triggered by RANKL is thus considered to be a crucial therapeutic objective for the treatment of postmenopausal osteoporosis (13).

Casticin (Cas) is a methoxy flavonoid compound obtained from *Vitex trifolia* with medicinal properties (14). Cas has been shown to possess anti-inflammatory and antitumor activities (15,16). In addition, Cas has been found to promote wound healing and to improve the symptoms of menopause in ovariectomized rats (17,18). Previous studies have demonstrated that osteoclast activity and osteolytic bone diseases are directly associated to inflammation (19,20). The aim of the present study was to ascertain whether Cas can affect the differentiation and function of osteoclasts, and explore its probable mechanisms of action, as its role in osteoclastogenesis has not yet been clarified. The protective effects of Cas in a mouse model of estrogen deficiency highlight its potential to prevent postmenopausal osteoporosis.

Materials and methods

Cell source and animal care. In this part of the experiment, 20 SPF grade C57BL/6 female mice aged 6-8 weeks and weighing ~20 g were obtained from the Animal Experiment Center of Guangxi Medical University (Nanning, China). The animal experiments were performed after approval (approval no. 202110004) from the Animal Care and Welfare Committee of Guangxi Medical University. The mice were euthanized after being suffocated with carbon dioxide at a displacement rate of 50%/min, the long bones of both lower limbs were removed, and the bone marrow cavities were rinsed with α-MEM (Thermo Fisher Scientific, Inc.) to collect cells. Mouse bone macrophage precursor cells were collected by flushing the bone marrow volume of all long bones and culturing for 4 days under complete medium [α-MEM, 1% penicillin/streptomycin-mixed antibiotics and 10% fetal bovine serum (FBS; Thermo Fisher Scientific, Inc.) conditions and 25 ng/ml M-CSF (R&D Systems, Inc.)], followed by digestion of the cells with trypsin for 5 min, centrifugation at 120 x g, at 25˚C for 5 min, and suspension counting, for use in subsequent experiments. The mice were maintained at the laboratory of pathogen-free animals of Guangxi Medical University under conditions of constant temperature at 25˚C, 60% constant humidity, 12 h of alternating light, unrestricted activity, and SPF-grade normal mouse chow available *ad libitum*. The cell culture conditions were a 37˚C constant temperature and a constant CO_2 concentration of 5%.

Antibodies and reagents. Cas (purity, ≥98%; purchased from Chengdu Must Biotechnology Co., Ltd.) was dissolved in dimethyl sulfoxide (DMSO) and diluted with α-MEM (Thermo Fisher Scientific, Inc.) to the desired experimental concentration. FBS was obtained from Thermo Fisher Scientific, Inc. MedChemExpress provided the CCK-8 kit. R&D Systems, Inc. provided recombinant mouse M-CSF and RANKL. Penicillin/streptomycin-mixed antibiotics, trypsin and bovine serum albumin (BSA) were from Gibco; Thermo Fisher Scientific, Inc. Rhodamine-phalloidin, DAPI, PBS, 4% paraformaldehyde tissue fixative, Triton X-100, β-estradiol and Alizarin Red S solution were purchased from Beijing Solarbio Science & Technology Co., Ltd., and Beyotime Institute of Biotechnology provided the alkaline phosphatase assay kit. Santa Cruz Biotechnology, Inc. provided the p65 fluorescent antibodies (cat. no. sc-8008 Alexa Fluor® 546; 1:100 dilution) used for p65 nuclear translocation, and the primary antibodies, NFATc1 (cat. no. sc7294; 1:200 dilution) and cathepsin K (CTSK; cat. no. sc-48353; 1:200 dilution), used for western blot analysis. Abcam provided the c-Fos antibody (cat. no. ab134122; 1:500 dilution). The majority of the remaining primary antibodies were produced by Cell Signaling Technology, Inc., including NF-κB p65 (product no. 8242; 1:1,000 dilution), phosphorylated (p)-p65 (product no. 3033; 1:1,000 dilution), NF-κB1 p105/p50 (product no. 13586; 1:1,000 dilution), IκBα (product no. 4812, 1:1,000 dilution), ERK1/2 (product no. 4695; 1:1,000 dilution), p-ERK1/2 (product no. 4370; 1:2,000 dilution), p38 (product no. 8690; 1:1,000 dilution), p-p38 (product no. 4511; 1:1,000 dilution), JNK (product no. 9252; 1:1,000 dilution), p-JNK (product no. 4668; 1:1,000 dilution), TAK1 (product no. 4505; 1:1,000 dilution), p-TAK1 (product no. 9339; 1:1,000 dilution), Akt (product no. 9272; 1:1,000 dilution), p-Akt (product no. 4060; 1:2,000 dilution), GSK3β (product no. 5676; 1:1,000 dilution) and p-GSK3β (product no. 9327; 1:1,000 dilution). T-75 aerated cell culture flasks, cell-grade sterilized 96-well cell culture plates, cell-grade sterilized 6-well cell culture plates, sterile centrifuge tubes, and bovine bone chips were purchased from Eppendorf.

Tartrate-resistant acid phosphatase (TRAP) staining and osteoclast differentiation. Bone marrow-derived macrophages (BMMs) were inoculated in 96-well plates at a density of $6x10^3$ cells/well and incubated overnight at 37˚C and 5% CO_2. Following attachment, the plate was transferred to a biosafety cabinet, and the required concentration of RANKL and Cas was prepared with pre-warmed medium. Apart from the negative control group, the positive control and drug intervention groups were treated with 50 ng/ml RANKL and 0, 0.5, 1, 1.5 or 2 μM Cas. At the aforementioned concentrations, once per day, the medium was changed. The plate was gently rinsed with PBS and fixed for 1 h at 25˚C with 4% paraformaldehyde following 5-7 days of cell culture. The cells were then incubated at 50 μl/well for 15 min with TRAP (Sigma-Aldrich; Merck KGaA) staining solution at room temperature. The BMMs were stimulated with 50 ng/ml RANKL in the presence of 2 μM Cas at three stages of osteoclast development, and control wells were set up and stained as described above. The 96-well plates were then photographed using Cytation 5 (BioTek Instruments, Inc.) and the number of osteoclasts were counted using ImageJ software 1.51 (National Institutes of Health, Bethesda, MD), followed by statistical analysis, specifying positive staining, with a nuclei number of ≥3 as valid counts.

Cytotoxicity assay. The BMMs were cultured in 96-well plates at a density of $6x10^3$ cells/well, as described above. The plates were incubated at 37˚C and 5% CO_2. The following day, Cas (0, 0.5, 1, 1.5, 2 or 2.5 μM) was added, and after 96 h, 10 μl CCK-8 reagent was added to each well and incubated for 2 h at 37˚C and 5% CO_2. A multimode microplate reader (Berthold Technologies Gmbh & Co. KG) was used to measure the absorbance values.

F-actin ring staining. The cell culture conditions were identical to those used in the osteoclast differentiation assay.

Table I. Primer sequences used in reverse transcription-quantitative PCR.

Gene	Forward primer (5'-3')	Reverse primer (5'-3')
Atp6v0d2	GTGAGACCTTGGAAGACCTGAA	GAGAAATGTGCTCAGGGGCT
Dcstamp	TCTGCTGTATCGGCTCATCTC	ACTCCTTGGGTTCCTTGCTT
Fos	CCAGTCAAGAGCATCAGCAA	AAGTAGTGCAGCCCGGAGTA
Nfatc1	GGTGCTGTCTGGCCATAACT	GAAACGCTGGTACTGGCTTC
Ctsk	AGGCGGCTATATGACCACTG	TCTTCAGGGCTTTCTCGTTC
Mmp9	GAAGGCAAACCCTGTGTT	AGAGTACTGCTTGCCCAGGA
β-actin	TCTGCTGGAAGGTGGACAGT	CCTCTATGCCAACACAGTGC

Atp6v0d2, ATPase H^+ transporting V0 subunit D2; *Dcstamp*, dendrocyte expressed seven transmembrane protein; *Nfatc1*, nuclear factor of activated T cells, cytoplasmic 1; *Ctsk*, cathepsin K; *Mmp9*, matrix metalloproteinase 9.

Following cell maturation, the cells were fixed for 1 h at 25˚C with 4% paraformaldehyde, permeabilized for 5 min with a 0.1% Trixon-100/PBS mixture, and incubated for 30 min with a 3% BSA/PBS mixture at room temperature. The plate was then incubated for 1 h at 25˚C with rhodamine-phalloidin at a concentration of 1:200 diluted with 0.2% BSA solution. Subsequently, the wells were washed with 0.2% BSA and stained for 5 min at 25˚C with a 1:1,000 DAPI/PBS mixture, excess liquid was discarded, and the cells were washed and photographed with a Cytation 5 imaging multimode reader.

Osteoclast acidification assay. To assess the effects of Cas on osteoclast acidification, acridine orange dye [3,6-bis(dimethylamino)acridine] (MedChemExpress) was used as previously describd (21). The osteoclasts were cultured in the presence or absence of 0, 1 or 2 μM Cas, and the culture conditions were the same as those aforementioned. The cells were incubated with a mixture of 0 μg/ml acridine orange and α-MEM for 15 min at 37˚C and 5% CO_2, and the 96-well plates washed with PBS were photographed with a Cytation 5 imaging multimode reader, and images of the wells were obtained and saved.

Bone resorption assay. Bovine bone slices were processed in advance; $1x10^5$ BMMs were inoculated in six-well plates, and RANKL (50 ng/ml) was added the following day. The formed osteoclasts were inoculated in 96-well plates and cultured with the addition of Cas (0, 1 or 2 μM). Following 1 h of fixation in 4% paraformaldehyde at room temperature, the bone sections were cleaned with a brush and imaged using a Regulus 8100 scanning electron microscope (Hitachi Corporation). ImageJ software 1.51 was used to analyze the areas of bone resorption.

Reverse transcription-quantitative PCR (RT-qPCR). For culture into osteoclasts, $1x10^5$ BMMs were added to six-well plates and subjected to Cas (0, 1 or 2 μM). Total RNA was extracted using TRIzol® reagent 5 days later, and cDNA was produced using a Revert-Aid RT kit (Thermo Fisher Scientific, Inc.). SYBR Green Master (Roche Diagnostics) dye was used for RT-qPCR. A real-time fluorescence quantitative PCR instrument was then used to determine the mRNA expression. The reaction system involved heating to 95˚C for denaturation and holding at 4˚C for 55 cycles (99˚C, 15 sec; 60˚C, 15 sec; 72˚C, 40 sec). *β-actin*, a housekeeping gene, was used to normalize the gene expression, and the $2^{-\Delta\Delta Cq}$ method was applied to analyze the data (22). The primer sequences used are listed in Table I.

Western blot analysis. To demonstrate the mechanisms through which Cas inhibits signaling pathways, the BMMs were seeded in six-well plates at a density of $5x10^5$ cells per well. Before being stimulated for 1 h with 2 μM Cas, the BMMs were starved with α-MEM for 3 h, and RANKL (50 ng/ml) stimulation was then applied for 0, 5, 10, 20, 30 and 60 min. The BMMs were inoculated at $1x10^5$ cells/well in six-well plates and stimulated for 1, 3 and 5 days with Cas (2 μM) and RANKL (50 ng/ml), followed by lysis of the cells using RIPA buffer (Beijing Kangwei Century Biotechnology Co., Ltd.) to extract the proteins and protein concentrations were assessed using a BCA kit (Beyotime Institute of Biotechnology). Subsequently, 10% gels were prepared according to the PAGE Gel Fast Preparation kit instructions (cat. no. PG112; Shanghai Epizyme Biomedical Technology Co., Ltd.), 40 μg of proteins were loaded per lane, which were separated using the 10% SDS-PAGE, before transfer of the isolated proteins onto nitrocellulose membranes and blocking with 5% skim milk powder for 1 h at room temperature. The membranes were incubated with primary antibodies diluted in 5% BSA-PBS for 18 h before being placed in cold storage (4˚C). The membranes were then incubated with the corresponding secondary antibodies [goat anti-rabbit/mouse IgG (H+L), DyLight 800 4xPEG, cat. nos. SA5-35571/SA5-35521, respectively, Invitrogen; Thermo Fisher Scientific, Inc.; diluted in 5% skim milk] the following day for 1 h at room temperature and imaged using an Image Quant LAS-4000 system (GE Healthcare; Cytiva) to observe the target bands. ImageJ software 1.51 was used for densitometric analysis.

p65 nuclear translocation. The BMMs were seeded in confocal culture dishes at a cell density of $1x10^5$ and starved with α-MEM for 3 h after 1 day, followed by Cas (2 μM) intervention for 1 h and RANKL stimulation for 10 min. The cells were then fixed with 4% paraformaldehyde for 10 min at 37˚C and 5% CO_2. This was followed by washing with PBS, dialysis with 0.1% Triton X-100 for 5 min, and sealing with 3% BSA for 30 min. The nuclei were stained with DAPI for 5 min

at 25˚C following incubation with p65 fluorescent antibodies diluted in 0.3% BSA-PBS according to the manufacturer's instructions at room temperature, and the 96-well plates were imaged using a Cytation 5 reader; images were obtained and stored. ImageJ software 1.51 was used for analysis.

Mouse model of ovariectomy. Ovariectomy and micro-computed tomography (micro-CT) were performed as previously described (23). A total of 30 female C57BL/6 mice, weighing ~20 g and aged 9 weeks, were purchased from GemPharmatech LLC., and were randomly assigned to one of five groups as follows: The sham-operated group, ovariectomized (OVX) group, estrogen [estradiol (E_2)] group, and the Cas (2.5 mg/kg) and Cas (5 mg/kg) treatment groups. The mice were maintained at the laboratory of pathogen-free animals of Guangxi Medical University under conditions of constant temperature at 25˚C, 60% constant humidity, 12 h of alternating light, unrestricted activity, and SPF-grade normal mouse chow available *ad libitum*. Following acclimatization, tribromoethanol (150 mg/kg) was injected intraperitoneally for bilateral ovariectomy, and at 1 week after surgery, mice in the treatment group were intraperitoneally injected with 2.5 or 5 mg/kg Cas, mice in the E_2 group were injected with 100 ng/kg E_2 and mice in the sham group and OVX group were injected with the same volume of normal saline as the treatment group, once every 2 days for 42 consecutive days. After 6 weeks, the mice were asphyxiated by carbon dioxide. The flow rate of CO_2 used for euthanasia was 50%/min, for a 10-liter volume chamber, using a flow rate of 5 liters per minute. Their lower limbs and viscera were fixed in 4% paraformaldehyde for 48 h at 25˚C, and their tibiae were examined using micro-CT (SCANO MEDICAL AG).

Micro-CT and histological analysis. The isolated whole left tibiae were imaged and quantified using micro-CT. The analysis method was the same as in that in a previous study (24). The following were the scanning parameters: 50 kV source voltage; 500 A source current; 0.5 mm Al filter; 9 m pixel size; 180 degree rotation step. The region of interest in the distal tibia was selected and Mimics 19.0 (Materialise) was used to perform 3D reconstruction. Using SkyScan CT software (version 1.15.22; Bruker), the 3D images were used to calculate bone volume/tissue volume (BV/TV), trabecular number (Tb.N), trabecular thickness (Tb.Th), and trabecular separation (Tb.Sp). The sample was fixed in 4% paraformaldehyde at 25˚C for 24 h and decalcified at a temperature of 4˚C for at least 2 weeks with 10% EDTA before being cut into 5-μm-thick slices for histological staining and analysis. Next, the sections were stained with hematoxylin and eosin (H&E) for 5 min or TRAP staining for 30 min at 25˚C. The heart, liver and kidney of mice were also stained with H&E staining after the same preprocessing. The images of sections were obtained using uSCOPE MXII-20 Digital Microscope Slide Scanner (Microscopes International) and analyzed using Bioquent Osteo software 2019 (BIOQUENT).

Osteoblast proliferation and differentiation. MC3T3-E1 cells (product code FH0384; Shanghai Fuheng Biotechnology Co., Ltd.) were removed from -80˚C for rewarming, and cultured with a mixture of 10% FBS, 1% penicillin/streptomycin antibiotics and DMEM for 48 h at 37˚C. The cells were then digested with EDTA-trypsin for 5 min when the culture flask was full, and centrifuged at 120 x g for 5 min at room temperature. The cells were then inoculated in a 48-well plate ($5x10^4$ cells/well) and Cas (0, 1 and 2 μM) was used to treat the cultured cells. After 7 days, the alkaline phosphatase (ALP) activity was determined using a BCIP/NBT alkaline phosphatase chromogenic kit (cat. no. C3206; Beyotime Institute of Biotechnology) for 15 min at room temperature. The cells were stained using Alizarin Red S solution kit (cat. no. G1452, Beijing Solarbio Science & Technology Co., Ltd.) for 15 min at 25˚C to observe the formation of bone nodules by a Cytation 5 reader, 21 days later.

Statistical analysis. The aforementioned experiments were performed three separate times, the results were input into Graphpad Prism 8.00 (GraphPad Software, Inc.) for analysis, and the findings are expressed as the mean ± standard deviation (SD). The comparison of multicomponent means was performed using unpaired Student's t-test or one-way ANOVA, followed by Tukey's post hoc analysis. A P-value <0.05 was considered to indicate a statistically significant difference.

Results

Cas inhibits RANKL-induced osteoclast differentiation. Cas (Fig. 1A) has been shown to exhibit anti-inflammatory properties (25). The present study thus investigated its role in osteoclast differentiation. *In vitro* experiments with TRAP staining revealed that with the increasing Cas concentration, the inhibition of RANKL-induced osteoclast differentiation was observed in a concentration-dependent manner (Fig. 1B and C). The viability of BMMs was not affected at this concentration range (Fig. 1D), particularly at 2 μM, where the inhibitory effect was particularly pronounced. In addition, during the 6 days of incubation of the BMMs with RANKL, which is the entire differentiation process of osteoclasts, Cas continued to inhibit osteoclast differentiation and was most effective in the early stages of differentiation (Fig. 1E and F). Mature osteoclasts can form an actin ring, which is essential for osteoclasts to perform their bone resorption functions (26). Herein, the F-actin belt formed by osteoclast differentiation was stained with rhodamine-phalloidin and it was found that the formation of the F-actin belt was significantly hindered by Cas (Fig. 1G and H).

Cas inhibits the acidification and bone resorption of osteoclasts. Osteoclast cytoplasmic protons are transported to confined areas to form an acidic extracellular microenvironment for bone resorption. The present study then determined the effects of Cas on bone resorption function by growing RANKL-stimulated osteoclasts in 96-well plates for 2 days, while intervening with Cas and staining with acridine orange. The results revealed a decrease in acid secretion from osteoclasts (Fig. 2A and B). In addition, RANKL-stimulated osteoclasts were grown on bone chips for 2 days with Cas concentrations of 1 and 2 μM, and under an electron microscope, the area of resorption pits on the bone surface appeared

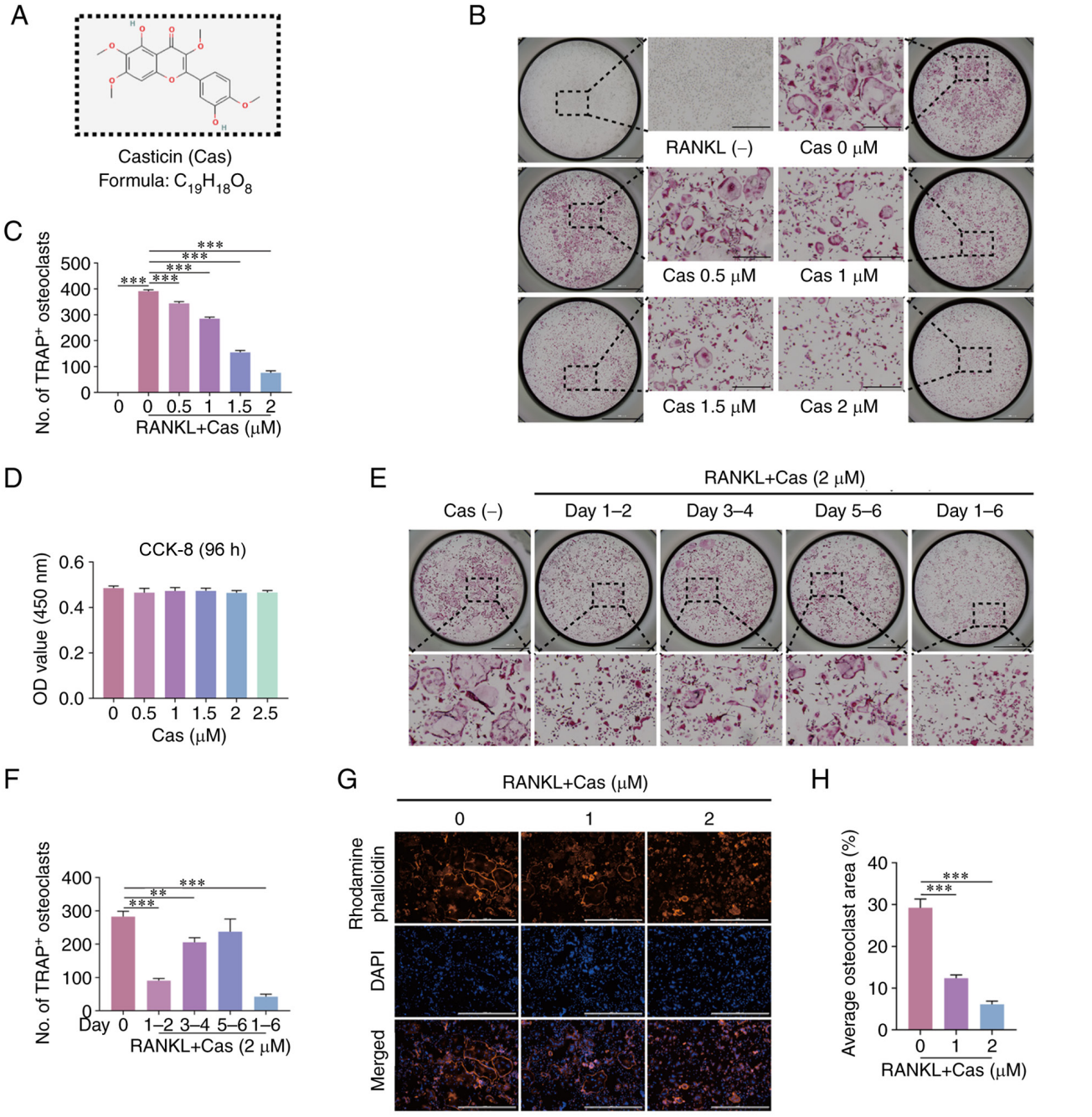

Figure 1. Cas inhibits receptor activator of nuclear factor κB ligand-induced osteoclast production. (A) Chemical structure of Cas. (B and C) The results of TRAP staining showed that Cas inhibited osteoclast formation in a concentration-dependent manner (osteoclasts were considered as mature when the number of nuclei was ≥3). The scale bar of the enlarged images is 500 μm. (D) The cytotoxicity of Cas on BMMs was assessed at 96 h using Cell Counting Kit-8 assay. (E and F) TRAP staining revealed the inhibitory effect of Cas in different stages of osteoclast formation. The scale bar of the enlarged images is 500 μm. (G and H) Immunofluorescence staining of F-actin belts in mature osteoclasts in the presence of different concentrations of Cas. The scale bar is 1,000 μm. **P<0.01 and ***P<0.001. All data are expressed as the mean ± SD. Cas, casticin; TRAP, tartrate-resistant acid phosphatase; RANKL, receptor activator of nuclear factor κB ligand; CCK-8, Cell Counting Kit-8.

to be reduced to varying degrees (Fig. 2C and D). These results verified that Cas inhibited the acid secretion and bone resorption function of osteoclasts.

Cas attenuates the expression of NFATc1, related genes and downstream proteins. The osteoclast differentiation process involves the expression of a series of specific genes that promote osteoclast maturation and bone resorption. The present study used RT-qPCR to detect osteoclast-specific gene expression under the influence of various concentrations of Cas. The results demonstrated that Cas inhibited the expression of osteoclast-specific genes, including *Nfatc1*, *Fos*, ATPase H^+ transporting V0 subunit D2 (*Atp6v0d2*), *Ctsk*, dendrocyte expressed seven transmembrane protein (*Dcstamp*) and matrix metalloproteinase 9 (*Mmp9*) (Fig. 3A-F). Subsequently, western blot analysis was used to examine the effects of Cas on the expression of NFATc1 and its downstream proteins. Cas treatment significantly reduced the protein expression levels

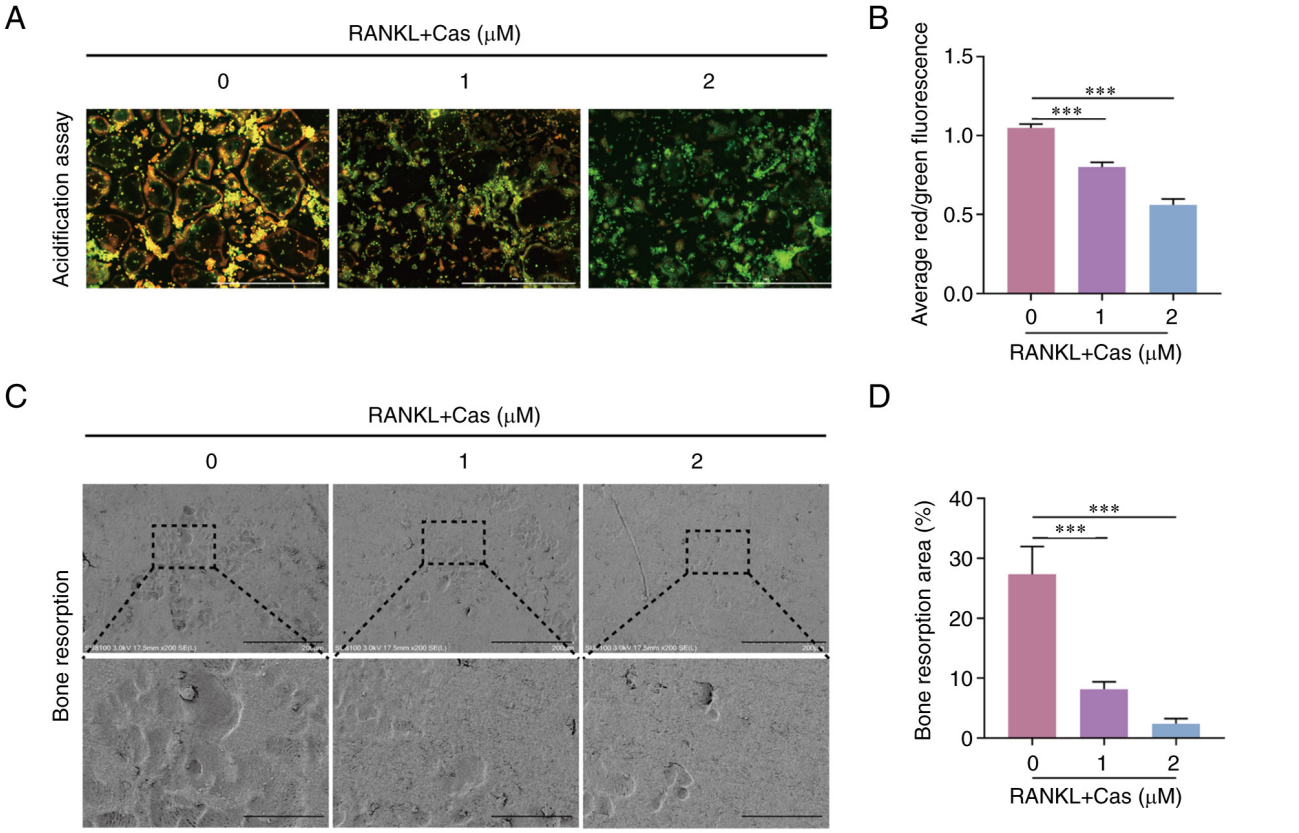

Figure 2. Cas inhibits osteoclast function. (A and B) Representative images revealed that the acidification function of osteoclasts was impaired after treatment with Cas at specified concentrations. Scale bar, 100 μm. (C and D) Representative images showed the inhibition of osteoclast resorption by Cas. Scale bar, 200 μm. ***P<0.001. All data are expressed as the mean ± SD. Cas, casticin; RANKL, receptor activator of nuclear factor κB ligand.

of NFATc1, c-Fos, CTSK and ATP6V0D2 (Fig. 3G-K). In summary, these findings indicated that Cas inhibited NFATc1 and downstream gene expression *in vitro*.

Cas inhibits the RANKL-induced activation of the AKT/ERK and NF-κB pathways. The main signaling pathways activated during osteoclastogenesis are considered to be NF-κB, MAPK and AKT (27). In the present study, to investigate the potential mechanisms affecting osteoclasts following Cas treatment, western blot analysis was used to examine the phosphorylation levels of signaling cascades for osteoclast differentiation. When the BMMs were stimulated with RANKL, p65 phosphorylation was inhibited. Immunofluorescence was also used to detect NF-κB p65 nuclear translocation (Fig. 4A and B). In addition, IκBα degradation was reduced following exposure to 2 μM Cas (Fig. 4C-E). The results revealed that various Cas concentrations significantly altered the nuclear translocation of p65. Moreover, Cas significantly inhibited ERK phosphorylation at 10 min (Fig. 5A and B), while JNK and p38 phosphorylation were unaffected. TAK1 belongs to the MAPK kinase family, and herein, it was verified that Cas had no significant effect on the phosphorylation of TAK1 upstream of the signaling pathway (Fig. S1). The AKT signaling pathway is also involved in osteoclast differentiation and survival (28). Cas inhibited the phosphorylation of AKT and GSK3β (Fig. 5A, C and D), a downstream signal of AKT. These findings indicated that Cas exerts an inhibitory effect on the activation of the AKT/ERK and NF-κB signaling pathways.

Cas reduces ovariectomy-induced bone loss in mice. To further investigate whether Cas can prevent osteoporosis, a mouse model of osteoporosis was employed using mice with devitalized ovaries. The mice were then injected 2.5 and 5 mg/kg Cas in the experimental group and with saline 100 ng/kg E_2 in the control group every 2 days for 42 days. No mortality or major adverse effects were observed during the surgery and the therapeutic intervention period. Cas had no significant toxic effects on the heart, liver, or kidneys, according to H&E staining (Fig. S2). Cas and E_2 prevented bone loss in mice compared with the control group (Fig. 6A), and quantitative analysis confirmed the trabecular parameters. BV/TV and Tb.N were significantly increased, Tb.sp was reduced in the experimental and E_2 groups when compared to the vehicle group (Fig. 6B-E). The amount of bone trabeculae was significantly higher in the Cas-treated animals, according to H&E staining (Fig. 6F and G). The groups treated with Cas had fewer osteoclasts, according to TRAP staining (Fig. 6H and I). These results further confirmed that Cas inhibits osteoclast formation and function *in vivo*.

Cas has no significant effect on osteoblasts in vitro. The present study also explored the effects of Cas on osteoblasts. MC3T3-E1 cells were cultured in the presence of Cas (1 and 2 μM). After 7 days of culture with osteoblast induction solution, the cells were stained with alkaline phosphatase and Alizarin Red S solutions after 21 days. Cas had no effect on the MC3T3-E1 cells (Fig. S3).

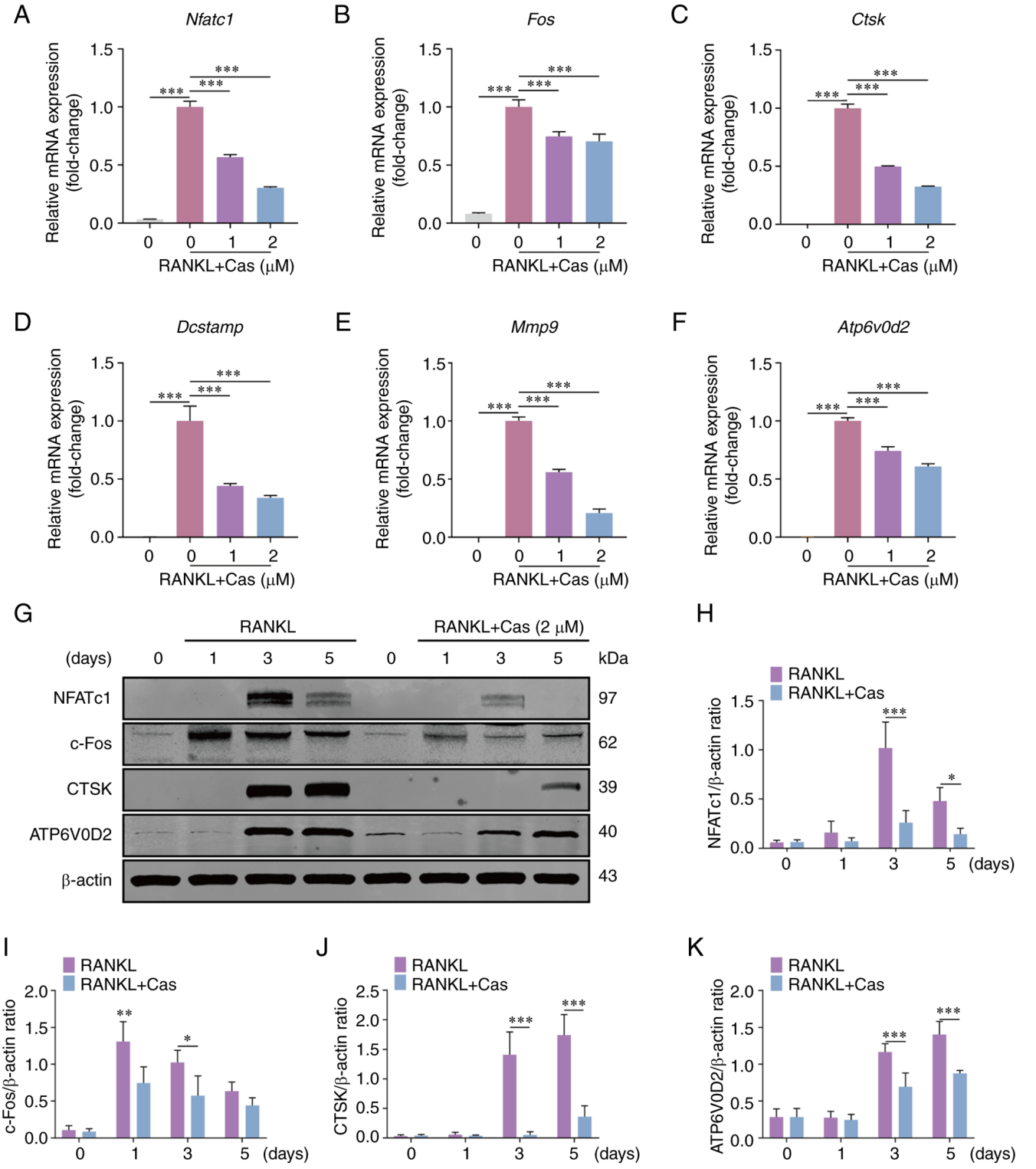

Figure 3. Cas inhibits the expression of NFATc1, downstream related genes and proteins. (A-F) Cas inhibited the expression of osteoclast-related genes *Nfatc1*, *Fos*, *Ctsk*, *Dcstamp*, *Mmp9* and *Atp6v0d2* stimulated by RANKL. (G) Typical western blot images of NFATc1, c-Fos, CTSK and ATP6V0D2 protein expression in osteoclasts stimulated by RANKL and 2 μM Cas for 0, 1, 3 and 5 days. (H-K) The relative ratio of the gray values of NFATc1, c-Fos, CTSK and ATP6V0D2 to β-actin was quantified. *P<0.05, **P<0.01 and ***P<0.001. All data are expressed as the mean ± SD. Cas, casticin; NFATc1, nuclear factor of activated T cells, cytoplasmic 1; *Ctsk*, cathepsin K; *Dcstamp*, dendrocyte expressed seven transmembrane protein; *Mmp9*, matrix metalloproteinase 9; *Atp6v0d2*, ATPase H^+ transporting V0 subunit D2; RANKL, receptor activator of nuclear factor κB ligand.

Discussion

The most common bone disease affecting women is postmenopausal osteoporosis. Estrogen deficiency causes excessive osteoclast activation and bone resorption, ultimately leading to a decrease in bone mass (29). Currently, there are a number of methods used to treat osteoporosis (30), and bisphosphonates are commonly used clinically, with considerable adverse

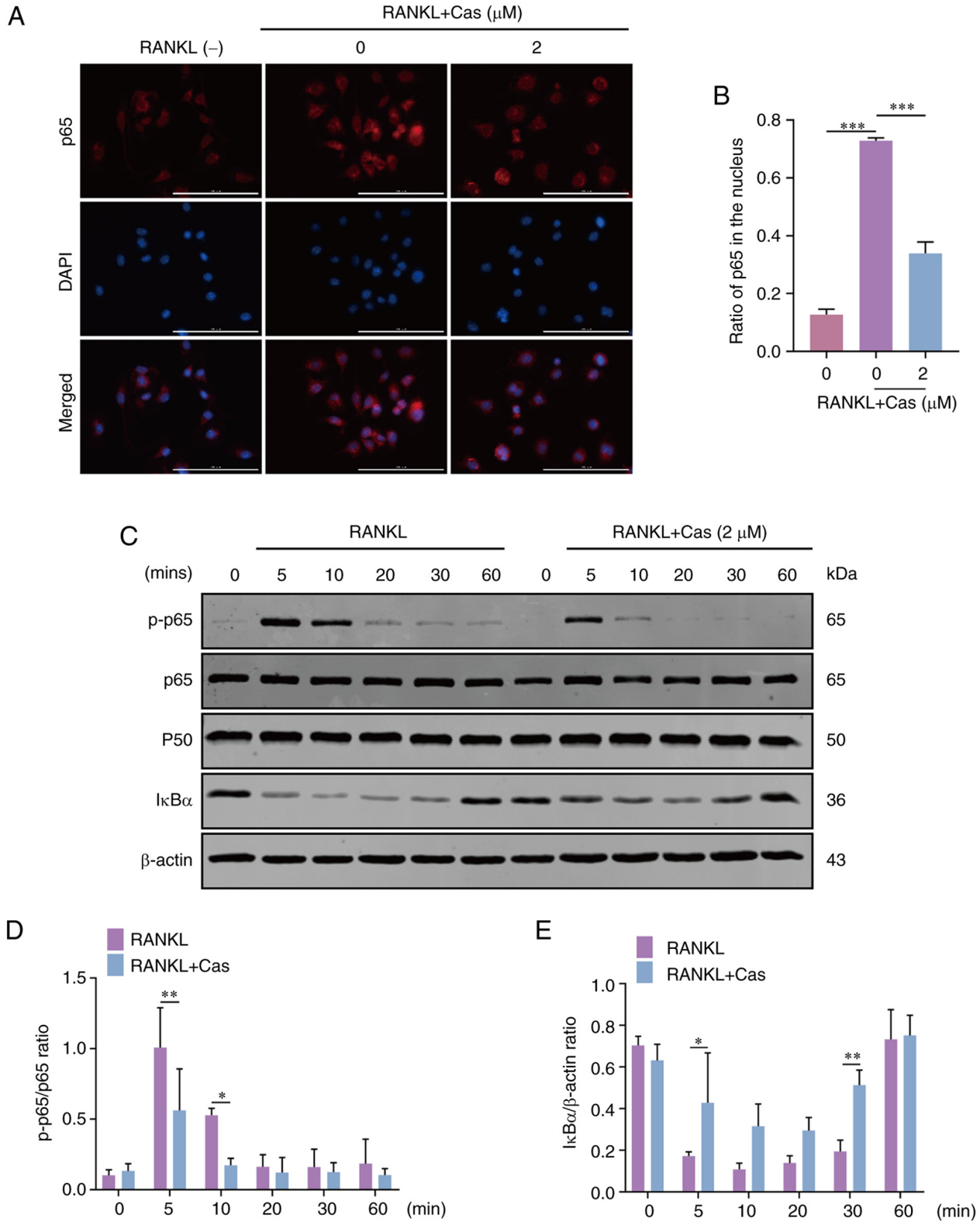

Figure 4. Cas inhibits the RANKL-induced NF-κB signaling pathway. (A) Cells from BMMs treated with RANKL and Cas were stained with p65 antibody and DAPI, and then images were captured under a fluorescence microscope. Scale bar, 100 μm. (B) Quantification of the rate of p65 into the nucleus. (C) Representative phosphorylated p65 and IκBα western blot images of Cas treated-BMMs at various time points. (D and E) The ratio of phosphorylated p65 to p65 and the ratio of IκBα to β-actin were quantified. *P<0.05, **P<0.01 and ***P<0.001. All data are expressed as the mean ± SD. Cas, casticin; RANKL, receptor activator of nuclear factor κB ligand; BMMs, bone marrow-derived macrophages; p-, phosphorylated.

effects, such as causing bone discontinuity after fracture and inhibiting bone formation (31). Therefore, the development of a class of drugs that are effective in the treatment of osteoporosis without severe side-effects is urgently required. The benefits of natural plant-based active components for safety over synthetic chemical medicines or estrogens are

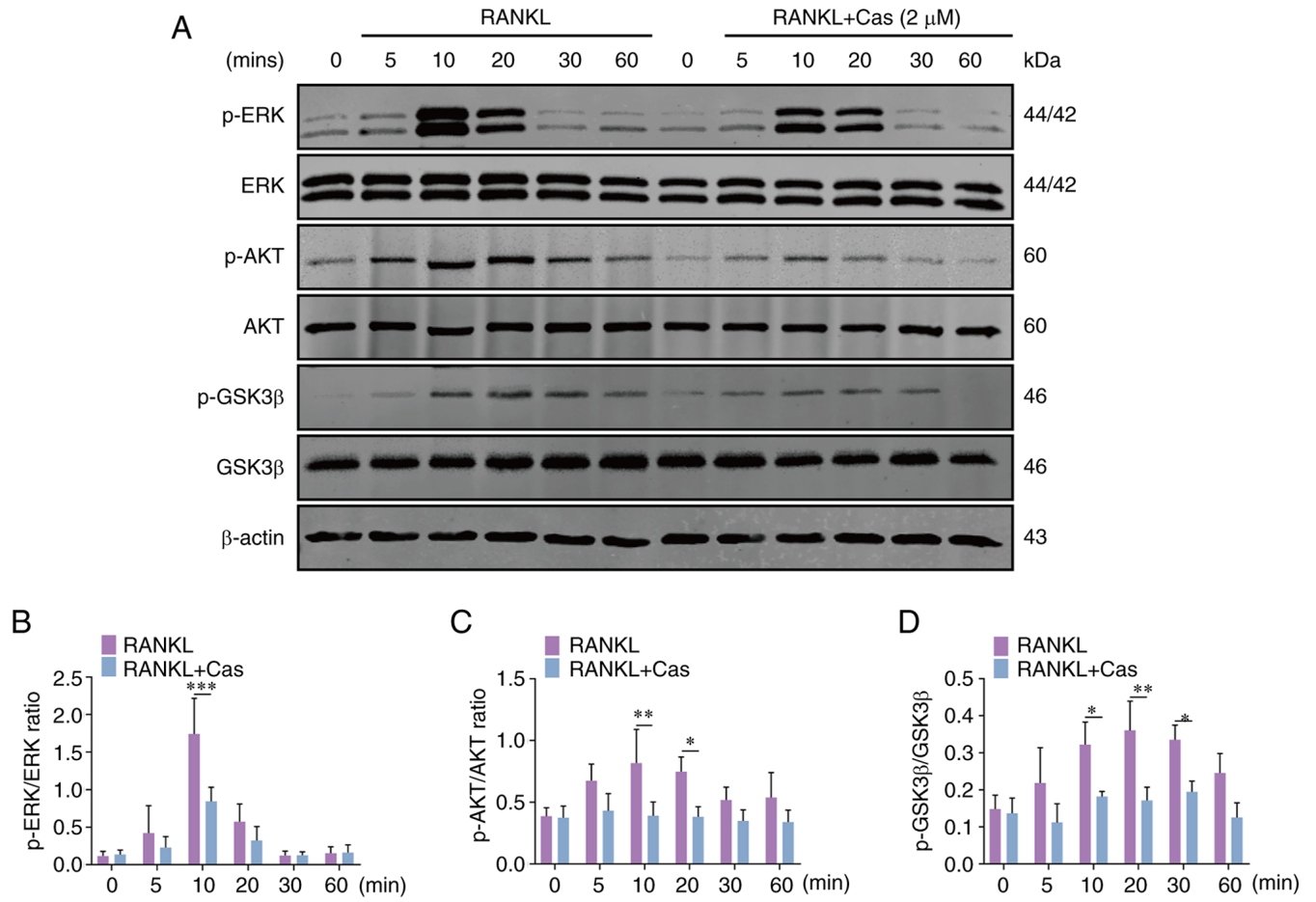

Figure 5. Cas inhibits the RANKL-induced ERK/AKT/GSK3β signaling pathway. (A) Effect of Cas on RANKL-induced ERK and AKT pathways. Specific antibodies were used to evaluate the protein expression and phosphorylation of ERK, AKT and GSK3β. (B-D) The ratio of quantified phosphorylated related proteins to corresponding total proteins is presented. *P<0.05, **P<0.01 and ***P<0.001. All data are expressed as the mean ± SD. Cas, casticin; RANKL, receptor activator of nuclear factor κB ligand; p-, phosphorylated.

more pronounced (32-34). Cas, as a natural compound with multiple pharmacological activities, has proven to be effective in several diseases and does not damage vital organs in mice (19,35,36). Bone mass is regulated by both osteoclasts and osteoblasts (37). The effects of Cas on osteoclast formation, fusion, and bone resorption capacity *in vitro*, as well as the osteoblast lineage, were investigated in the present study, while *in vivo*, the biological effects of Cas were examined on ovariectomy-induced osteoporosis. Cas inhibited osteoclast formation by suppressing the activation of the AKT/ERK and NF-κB pathways. As a result, *in vivo* analyses revealed that Cas inhibited the bone loss caused by a lack of estrogen.

Multiple cytokines, including RANKL and M-CSF, stimulate osteoclast differentiation, both of which lead to the activation of associated signaling cascades by binding to their downstream receptors to promote osteoclast activation (38). RANKL triggers the activation of downstream pathways through RANK signaling, followed by TRAF6 and downstream molecules, including NF-κB, MAPK, AKT-GSK3β, etc., all of which play critical roles in osteoclast development (39-41). During osteoclast differentiation, the phosphorylation of p65 and the degradation of the IκBα via proteasomes can result in the nuclear dimerization of p50 and p65/RelA. The activation of ERK in the MAPK pathway is also essential for osteoclast survival (42). Herein, Cas was found to hinder osteoclast differentiation and activation by affecting the phosphorylation of p65 and nuclear localization, the degradation of IκBα, as well as the phosphorylation of ERK. In comparison, TAK1 is a member of the MAPK kinase family (43), and Cas had no effect on the phosphorylation of TAK1.

A crucial transcription factor for osteoclasts is NFATc1 (44), of which a high expression is regulated by NF-κB and c-Fos. The persistent production of c-Fos is supported by the phosphorylation of ERK, which in turn stimulates NFATc1 in osteoclast progenitors and ultimately results in osteoclastogenesis (45). According to previous research, AKT promoted the formation of the inactive form of GSK3β (p-GSK3β), as well as the nuclear localization of NFATc1, whereas constitutively active GSK3β overexpression inhibited osteoclast formation by downregulating NFATc1 (46-48). The results of the present study demonstrated that Cas inhibited the phosphorylation of AKT/GSK3β and thus prevented the expression of related proteins and transcription factors required for osteoclast maturation, as well as the expression of the osteoclast-associated genes, *Nfatc1, Fos, Atp6v0d2, Ctsk, Dcstamp,* and *Mmp9* (Fig. 7), which are directly or indirectly regulated by NFATc1 (49).

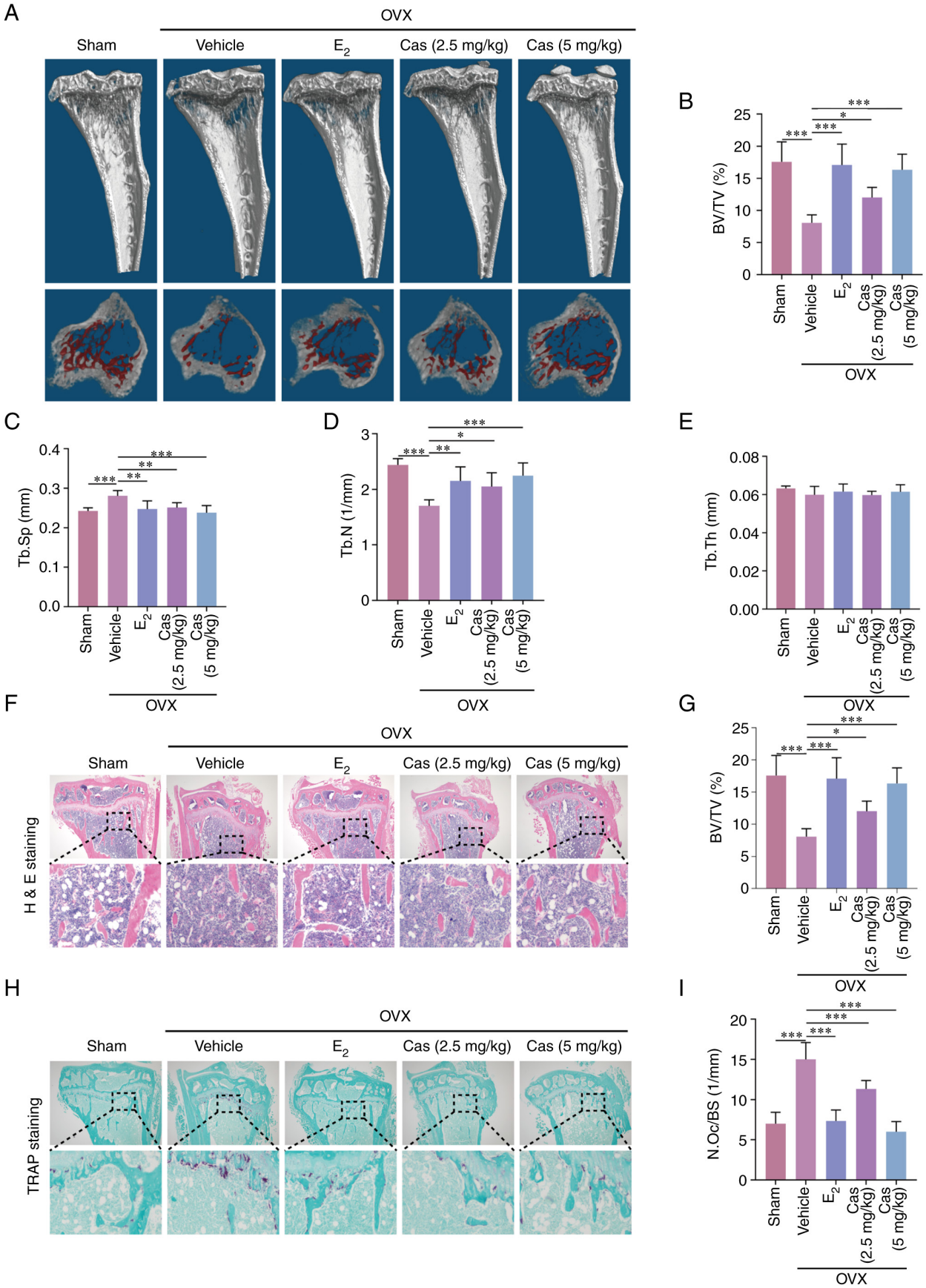

Figure 6. Casticin inhibits ovariectomized-induced bone loss. (A) 3D representative images of different groups of tibial plateau of mice. (B-E) Tibial cancellous bone data of BV/TV, trabecular separation, trabecular number, and trabecular thickness (n=6). (F) Representative H&E staining results of tibial plateau sections. (G) Quantification of H&E staining BV/TV in tibial plateau. (H) Representative TRAP staining results of tibial plateau sections. (I) Quantification of the number of osteoclasts in tibial plateau after TRAP staining. *P<0.05, **P<0.01 and ***P<0.001. All data are expressed as the mean ± SD. BV/TV, volume/tissue volume; H&E, hematoxylin and eosin; TRAP, tartrate-resistant acid phosphatase; OVX, ovariectomized; E_2, estradiol; Cas, casticin; Tb.Sp, trabecular separation; Tb.N, trabecular number; Tb.Th, trabecular thickness.

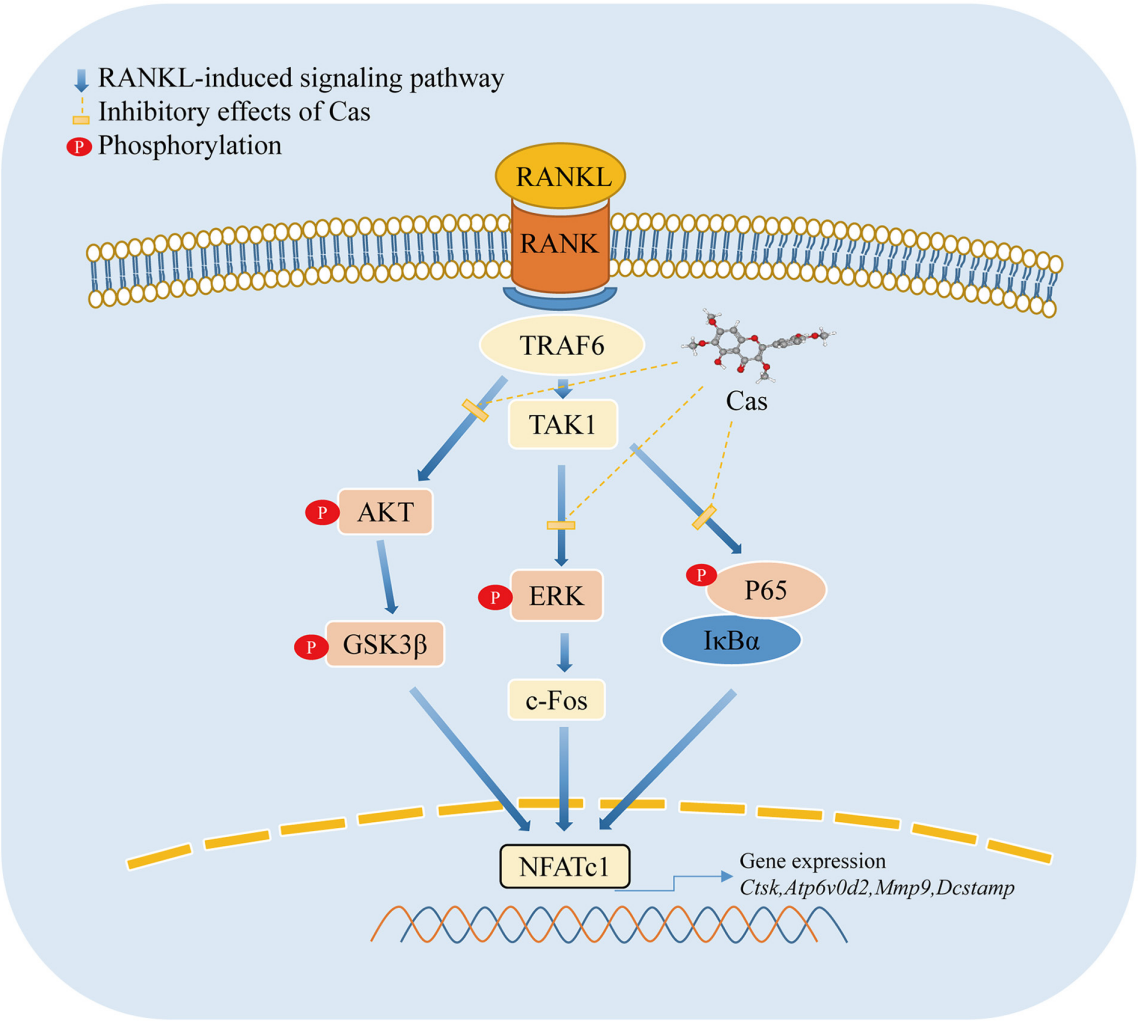

Figure 7. Working model of how Cas regulates osteoclastogenesis. Cas negatively regulates osteoclast differentiation through the receptor activator of nuclear factor κB ligand-induced AKT/ERK/NF-κB pathway to control osteoclastogenesis-related transcriptional processes and genes expression. Cas, casticin; RANKL, receptor activator of nuclear factor κB ligand; NFATc1, nuclear factor of activated T cells, cytoplasmic 1; *Ctsk*, cathepsin K; *Atp6v0d2*, ATPase H^+ transporting V0 subunit D2; *Mmp9*, matrix metalloproteinase 9; *Dcstamp*, dendrocyte expressed seven transmembrane protein.

There are some limitations to the present study. The study explored the mechanism by which Cas inhibits osteoclast activation, which has been shown to be multi-pathway. Studies on NF-κB, MAPK, AKT and other conventional pathways have been widely carried out (27,50), and most studies use pathway inhibitors as experimental controls (51-53), thus, in the future, the mechanism of Cas inhibition of osteoclast activation using inhibitors of the ERK/AKT/GSK3β pathway will be further investigated. The association between the Cas-inhibited RANKL-induced ERK/AKT/GSK3β signaling pathway and NFATc1 and its downstream proteins requires further study. Notably, the molecular mechanism of Cas inhibition needs further study *in vivo*. Cas has recently been reported to inhibit reactive oxygen species (ROS) to reduce cartilage degeneration associated with osteoarthritis (54), and whether there is a link with ROS clearance in osteoclasts and bone cells needs to be further investigated. Cas also plays a role in oncological disease, and its role in tumor bone metastasis may represent an interest of future investigation.

In conclusion, the results of the present study demonstrated that Cas prevents ovariectomy-induced bone loss by suppressing the effects of RANKL on osteoclast differentiation and function via regulating the AKT/ERK and NF-κB signaling pathways. Thus, Cas may have potential for use as a therapeutic agent for the prevention of postmenopausal osteoporosis.

Acknowledgements

Not applicable.

Funding

The present study was funded by the National Natural Science Foundation of China (grant no. 81960405), and the Guangxi Science, Technology Base and Talent Special Project (grant no. GuikeAD 19254003).

Availability of data and materials

The analyzed data sets generated during the present study are available from the corresponding author on reasonable request.

Authors' contributions

JZ, QL and JX conceived and designed the study. FY and YS drafted the manuscript and performed the experiments. JL and KW performed the experiments. HL and JC acquired and analyzed the data. JX revised the manuscript. All of the authors confirm the authenticity of all the raw data. All authors read and approved the manuscript and agree to be accountable for all aspects of the research in ensuring that the accuracy or integrity of any part of the work are appropriately investigated and resolved.

Ethics approval and consent to participate

The animal experiments were performed after approval (approval no. 202110004) from the Animal Care and Welfare Committee of Guangxi Medical University (Nanning, China).

Patient consent for publication

Not applicable.

Competing interests

The authors declare that they have no competing interests.

References

1. Michalski MN and McCauley LK: Macrophages and skeletal health. Pharmacol Ther 174: 43-54, 2017.
2. Boyle WJ, Simonet WS and Lacey DL: Osteoclast differentiation and activation. Nature 423: 337-342, 2003.
3. Kular J, Tickner J, Chim SM and Xu J: An overview of the regulation of bone remodelling at the cellular level. Clin Biochem 45: 863-873, 2012.
4. Sobh MM, Abdalbary M, Elnagar S, Nagy E, Elshabrawy N, Abdelsalam M, Asadipooya K and El-Husseini A: Secondary osteoporosis and metabolic bone diseases. J Clin Med 11: 2382, 2022.
5. Han Y, You X, Xing W, Zhang Z and Zou W: Paracrine and endocrine actions of bone-the functions of secretory proteins from osteoblasts, osteocytes, and osteoclasts. Bone Res 6: 16, 2018.
6. Bae SJ, Shin MW, Son T, Lee HS, Chae JS, Jeon S, Oh GT and Kim KW: Ninjurin1 positively regulates osteoclast development by enhancing the survival of prefusion osteoclasts. Exp Mol Med 51: 1-16, 2019.
7. Chen K, Qiu P, Yuan Y, Zheng L, He J, Wang C, Guo Q, Kenny J, Liu Q, Zhao J, *et al*: Pseurotin A inhibits osteoclastogenesis and prevents ovariectomized-induced bone loss by suppressing reactive oxygen species. Theranostics 9: 1634-1650, 2019.
8. Sun Y, Li J, Xie X, Gu F, Sui Z, Zhang K and Yu T: Macrophage-osteoclast associations: Origin, polarization, and subgroups. Front Immunol 12: 778078, 2021.
9. Tobeiha M, Moghadasian MH, Amin N and Jafarnejad S: RANKL/RANK/OPG pathway: A mechanism involved in exercise-induced bone remodeling. Biomed Res Int 2020: 6910312, 2020.
10. Asagiri M and Takayanagi H: The molecular understanding of osteoclast differentiation. Bone 40: 251-264, 2007.
11. Takayanagi H: The role of NFAT in osteoclast formation. Ann N Y Acad Sci 1116: 227-237, 2007.
12. Grigoriadis AE, Wang ZQ, Cecchini MG, Hofstetter W, Felix R, Fleisch HA and Wagner EF: c-Fos: A key regulator of osteoclast-macrophage lineage determination and bone remodeling. Science 266: 443-448, 1994.
13. Bellavia D, Dimarco E, Costa V, Carina V, De Luca A, Raimondi L, Fini M, Gentile C, Caradonna F and Giavaresi G: Flavonoids in bone erosive diseases: Perspectives in osteoporosis treatment. Trends Endocrinol Metab 32: 76-94, 2021.
14. Mesaik MA, Murad S, Khan KM, Tareen RB, Ahmed A and Choudhary MI: Isolation and immunomodulatory properties of a flavonoid, casticin from *Vitex agnus-castus*. Phytother Res 23: 1516-1520, 2009.
15. Chan EWC, Wong SK and Chan HT: Casticin from Vitex species: A short review on its anticancer and anti-inflammatory properties. J Integr Med 16: 147-152, 2018.
16. Ramchandani S, Naz I, Lee JH, Khan MR and Ahn KS: An overview of the potential antineoplastic effects of casticin. Molecules 25: 1287, 2020.
17. Sun C, Yan H, Jiang K and Huang L: Protective effect of casticin on experimental skin wound healing of rats. J Surg Res 274: 145-152, 2022.
18. Lee JH, Lee S, Nguyen QN, Phung HM, Shin MS, Kim JY, Choi H, Shim SH and Kang KS: Identification of the active ingredient and beneficial effects of *Vitex rotundifolia* fruits on menopausal symptoms in ovariectomized rats. Biomolecules 11: 1033, 2021.
19. Li J, Qiu C, Xu P, Lu Y and Chen R: Casticin improves respiratory dysfunction and attenuates oxidative stress and inflammation via inhibition of NF-κB in a chronic obstructive pulmonary disease model of chronic cigarette Smoke-exposed rats. Drug Des Devel Ther 14: 5019-5027, 2020.
20. Xu J, Wu HF, Ang ES, Yip K, Woloszyn M, Zheng MH and Tan RX: NF-kappaB modulators in osteolytic bone diseases. Cytokine Growth Factor Rev 20: 7-17, 2009.
21. Qin A, Cheng TS, Lin Z, Pavlos NJ, Jiang Q, Xu J, Dai KR and Zheng MH: Versatile roles of V-ATPases accessory subunit Ac45 in osteoclast formation and function. PLoS One 6: e27155, 2011.
22. Livak KJ and Schmittgen TD: Analysis of relative gene expression data using real-time quantitative PCR and the 2(-Delta Delta C(T)) method. Methods 25: 402-408, 2001.
23. Xiao L, Zhong M, Huang Y, Zhu J, Tang W, Li D, Shi J, Lu A, Yang H, Geng D, *et al*: Puerarin alleviates osteoporosis in the ovariectomy-induced mice by suppressing osteoclastogenesis via inhibition of TRAF6/ROS-dependent MAPK/NF-κB signaling pathways. Aging (Albany NY) 12: 21706-21729, 2020.
24. Sapra L, Shokeen N, Porwal K, Saini C, Bhardwaj A, Mathew M, Mishra PK, Chattopadhyay N, Dar HY, Verma B and Srivastava RK: *Bifidobacterium longum* ameliorates ovariectomy-induced bone loss via enhancing anti-osteoclastogenic and immunomodulatory potential of regulatory B cells (Bregs). Front Immunol 13: 875788, 2022.
25. Li X, Mei W, Huang Z, Zhang L, Zhang L, Xu B, Shi X, Xiao Y, Ma Z, Liao T, *et al*: Casticin suppresses monoiodoacetic acid-induced knee osteoarthritis through inhibiting HIF-1α/NLRP3 inflammasome signaling. Int Immunopharmacol 86: 106745, 2020.
26. Teitelbaum SL: Bone resorption by osteoclasts. Science 289: 1504-1508, 2000.
27. Pereira M, Petretto E, Gordon S, Bassett JHD, Williams GR and Behmoaras J: Common signalling pathways in macrophage and osteoclast multinucleation. J Cell Sci 131: jcs216267, 2018.
28. Adamik J, Pulugulla SH, Zhang P, Sun Q, Lontos K, Macar DA, Auron PE and Galson DL: EZH2 supports osteoclast differentiation and bone resorption via epigenetic and cytoplasmic targets. J Bone Miner Res 35: 181-195, 2020.
29. Khosla S, Oursler MJ and Monroe DG: Estrogen and the skeleton. Trends Endocrinol Metab 23: 576-581, 2012.
30. Song S, Guo Y, Yang Y and Fu D: Advances in pathogenesis and therapeutic strategies for osteoporosis. Pharmacol Ther 237: 108168, 2022.
31. Kim HS, Jung HY, Kim MO, Joa KL, Kim YJ, Kwon SY and Kim CH: Successful conservative treatment: Multiple atypical fractures in osteoporotic patients after bisphosphate medication: A unique case report. Medicine (Baltimore) 94: e446, 2015.
32. Yang X, Liang J, Wang Z, Su Y, Zhan Y, Wu Z, Li J, Li X, Chen R, Zhao J, *et al*: Sesamolin protects mice from ovariectomized bone loss by inhibiting osteoclastogenesis and RANKL-mediated NF-κB and MAPK signaling pathways. Front Pharmacol 12: 664697, 2021.
33. Xian Y, Su Y, Liang J, Long F, Feng X, Xiao Y, Lian H, Xu J, Zhao J, Liu Q and Song F: Oroxylin A reduces osteoclast formation and bone resorption via suppressing RANKL-induced ROS and NFATc1 activation. Biochem Pharmacol 193: 114761, 2021.
34. Ding D, Yan J, Feng G, Zhou Y, Ma L and Jin Q: Dihydroartemisinin attenuates osteoclast formation and bone resorption via inhibiting the NF-κB, MAPK and NFATc1 signaling pathways and alleviates osteoarthritis. Int J Mol Med 49: 4, 2022.
35. Kowalski M, Assa A, Patil K, Terrell C, Holliday N and Pai SB: Casticin impacts key signaling pathways in colorectal cancer cells leading to cell death with therapeutic implications. Genes (Basel) 13: 815, 2022.
36. Fan L, Zhang Y, Zhou Q, Liu Y, Gong B, Lü J, Zhu H, Zhu G, Xu Y and Huang G: Casticin inhibits breast cancer cell migration and invasion by down-regulation of PI3K/Akt signaling pathway. Biosci Rep 38: BSR20180738, 2018.

37. Wang L, You X, Zhang L, Zhang C and Zou W: Mechanical regulation of bone remodeling. Bone Res 10: 16, 2022.
38. Takayanagi H: RANKL as the master regulator of osteoclast differentiation. J Bone Miner Metab 39: 13-18, 2021.
39. Sun Y, Li J, Xie X, Gu F, Sui Z, Zhang K and Yu T: Recent advances in osteoclast biological behavior. Front Cell Dev Biol 9: 788680, 2021.
40. Novack DV: Role of NF-κB in the skeleton. Cell Res 21: 169-182, 2011.
41. Cao H, Zhu K, Qiu L, Li S, Niu H, Hao M, Yang S, Zhao Z, Lai Y, Anderson JL, *et al*: Critical role of AKT protein in myeloma-induced osteoclast formation and osteolysis. J Biol Chem 288: 30399-30410, 2013.
42. Soysa NS, Alles N, Aoki K and Ohya K: Osteoclast formation and differentiation: an overview. J Med Dent Sci 59: 65-74, 2012.
43. Jo YJ, Lee HI, Kim N, Hwang D, Lee J, Lee GR, Hong SE, Lee H, Kwon M, Kim NY, *et al*: Cinchonine inhibits osteoclast differentiation by regulating TAK1 and AKT, and promotes osteogenesis. J Cell Physiol 236: 1854-1865, 2021.
44. Sitara D and Aliprantis AO: Transcriptional regulation of bone and joint remodeling by NFAT. Immunol Rev 233: 286-300, 2010.
45. Xu W, Chen X, Wang Y, Fan B, Guo K, Yang C, Yu S, Pang Y and Zhang S: Chitooligosaccharide inhibits RANKL-induced osteoclastogenesis and ligation-induced periodontitis by suppressing MAPK/ c-fos/NFATC1 signaling. J Cell Physiol 235: 3022-3032, 2020.
46. Zhang Q, Hu S, He Y, Song Z, Shen Y, Zhao Z, Zhang Q, Qin L and Zhang Q: Monotropein protects against inflammatory bone loss and suppresses osteoclast formation and bone resorption by inhibiting NFATc1 via NF-κB and Akt/GSK-3β pathway. Nutrients 14: 3978, 2022.
47. Fan X, Xiong H, Wei J, Gao X, Feng Y, Liu X, Zhang G, He QY, Xu J and Liu L: Cytoplasmic hnRNPK interacts with GSK3β and is essential for the osteoclast differentiation. Sci Rep 5: 17732, 2015.
48. Yang S, Song D, Wang Z, Su Y, Chen J, Xian Y, Huang J, Li J, Xu J, Zhao J and Liu Q: AKT/GSK3β/NFATc1 and ROS signal axes are involved in AZD1390-mediated inhibitory effects on osteoclast and OVX-induced osteoporosis. Int Immunopharmacol 113: 109370, 2022.
49. Song I, Kim JH, Kim K, Jin HM, Youn BU and Kim N: Regulatory mechanism of NFATc1 in RANKL-induced osteoclast activation. FEBS Lett 583: 2435-2440, 2009.
50. Meng B, Wu D, Cheng Y, Huang P, Liu Y, Gan L, Liu C and Cao Y: Interleukin-20 differentially regulates bone mesenchymal stem cell activities in RANKL-induced osteoclastogenesis through the OPG/RANKL/RANK axis and the NF-κB, MAPK and AKT signalling pathways. Scand J Immunol 91: e12874, 2020.
51. Jiang T, Gong Y, Zhang W, Qiu J, Zheng X, Li Z, Yang G and Hong Z: PD0325901, an ERK inhibitor, attenuates RANKL-induced osteoclast formation and mitigates cartilage inflammation by inhibiting the NF-κB and MAPK pathways. Bioorg Chem 132: 106321, 2023.
52. Lee ZH, Lee SE, Kim CW, Lee SH, Kim SW, Kwack K, Walsh K and Kim HH: IL-1alpha stimulation of osteoclast survival through the PI 3-kinase/Akt and ERK pathways. J Biochem 131: 161-166, 2002.
53. Chaisson ML, Branstetter DG, Derry JM, Armstrong AP, Tometsko ME, Takeda K, Akira S and Dougall WC: Osteoclast differentiation is impaired in the absence of inhibitor of kappa B kinase alpha. J Biol Chem 279: 54841-54848, 2004.
54. Chu J, Yan B, Zhang J, Peng L, Ao X, Zheng Z, Jiang T and Zhang Z: Casticin attenuates osteoarthritis-related cartilage degeneration by inhibiting the ROS-Mediated NF-κB signaling pathway in vitro and in vivo. Inflammation 43: 810-820, 2020.